Journal of Sound and Vibration (2002) **249**(1), 41–53
doi:10.1006/jsvi.2001.3801, available online at http://www.idealibrary.com on IDEAL®

INFLUENCE OF A LEVELNESS DEFECT IN A THRUST BEARING ON THE DYNAMIC BEHAVIOUR OF AN ELASTIC SHAFT

S. Berger, O. Bonneau and J. Frêne

Laboratoire de Mécanique des Solides SP2MI-Bd 3-*Teléport* 2-*BP* 179-86960
FUTUROSCOPE Cedex France. E-mail: sh.berger@essaim.univ-mulhouse.fr

(*Received* 18 *October* 1999, *and in final form* 2 *April* 2001)

This paper examines the non-linear dynamic behaviour of a flexible shaft. The shaft is mounted on two journal bearings and the axial load is supported by a defective hydrodynamic thrust bearing at one end. The defect is a levelness defect of the rotor. The thrust bearing behaviour must be considered to be non-linear because of the effects of the defect. The shaft is modelled with typical beam finite elements including effects such as the gyroscopic effects. A modal technique is used to reduce the number of degrees of freedom. Results show that the thrust bearing defects introduce supplementary critical speeds. The linear approach is unable to show the supplementary critical speeds which are obtained only by using non-linear analysis.

1. INTRODUCTION

The economical constraints of industry oblige manufacturers to increase the capabilities of their plants. In the turbomachinery field the rule is the same. Mechanisms such as turbines or pumps are used in more and more exacting conditions: higher operating speeds, pressures and charges. Engineers must design these types of rotating machinery to very high accuracy.

The dynamic behaviour of the shaft depends strongly on elements surrounding the shaft such as squeeze film dampers, journal bearings and thrust bearings. However, these surrounding elements might also have some manufacturing defects. It is important to consider these defects because they might generate poor dynamic behaviour of the rotating machinery. In hydrodynamic lubrication, the film thickness can be very small and the rotor defects can induce important variations of the pressure field. The study of defect bearings has been carried out by several authors and the objectives of these studies were to evaluate the minimum film thickness. Fantino [1], Fantino and Frêne [2] and Berthe *et al.* [3] presented studies on the influence of the shape defects and surface roughness on the hydrodynamics of lubricated systems. They have particularly shown that the Reynolds equation was not applicable when the defects are significant and instead, the viscous thin film equation developed by Berthe and Godet has to be used [4]. Some studies have been carried out on the influence of a defective journal bearing on the dynamic behaviour of a flexible shaft. Bonneau and Frêne [5] have shown, through linear calculations that a defective journal bearing can create a dynamic perturbation of an unpredictable frequency. The defect can excite the critical speeds even if there are no imbalance forces. Some studies have been carried out on the action of a thrust bearing on lateral shaft

0022-460X/02/010041 + 13 $35.00/0

vibrations [6, 7]. These authors have shown that the influence of a thrust bearing may be significant and positive. Berger *et al.* [8] have studied in particular the effects of the non-linear dynamic behaviour of a defective thrust bearing on the bending vibrations of a flexible shaft. The defect was defined as an angle between the rotation axis of the shaft and the normal vector of the rotor. The axial dynamic behaviour of the shaft was not considered. They have shown that, even without an imbalance force, a small defect on the thrust bearing rotor excites the first critical speed. The response is similar to an imbalance response. Another domain of defect bearing study is the defects due to the elastic deformation of contact surfaces. This has been developed in the field of connecting rod bearings of petrol and diesel engines [9–13]. These deformations are induced by the large value of load resulting from the high hydrodynamic pressure due to the explosion and the connecting rod inertia. This elastohydrodynamic problem is one of the simultaneous approaches of pressure field computation and deformation field calculation.

The aim of this paper is to study the non-linear effects of a defective thrust bearing on the dynamic behaviour of a flexible shaft. The defect is a wave on the rotor surface due to a manufacturing problem. Both the axial and the bending behaviour of the rotor are taken into account.

2. THEORY

2.1. THRUST BEARING

2.1.1. *Model*

The thrust bearing has four fixed pads. Figure 1 represents the hydrodynamic thrust bearing model. (o_0, x_0, y_0, z_0) is the fixed reference, (o_1, x_1, y_1, z_1) and (o_2, x_2, y_2, z_2) are,

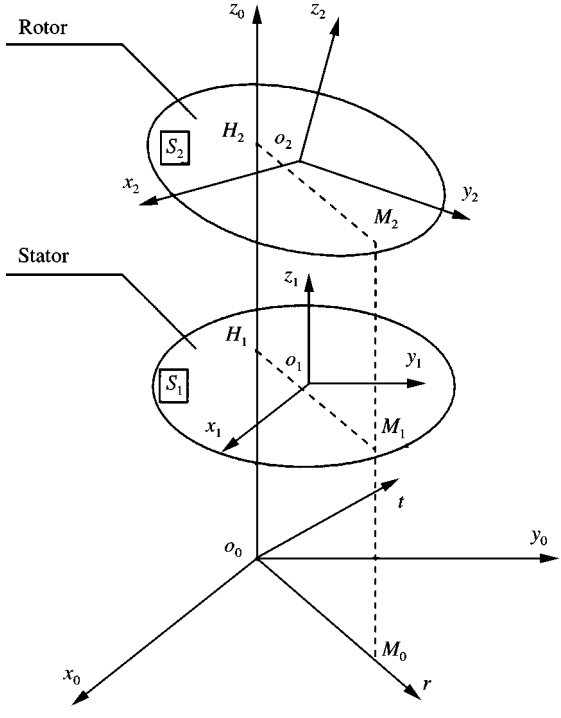

Figure 1. Thrust bearing scheme.

respectively, fixed to the centre o_1 of the stator and the centre o_2 of the rotor. The rotor has three translations in the directions, x_0, y_0 and z_0 and two misalignment angles (x_2- and y_2-axis). z_2 is the axis of rotation of the rotor.

In the cylindrical reference $(0_0, r, t, z_0)$, the thin film equation is defined by

$$\frac{\partial}{\partial r}\left(rh^3\frac{\partial p}{\partial r}\right)+\frac{\partial}{\partial \theta}\left(\frac{h^3}{r}\frac{\partial p}{\partial \theta}\right)=-6\mu r U_2\frac{\partial h}{\partial r}-6\mu V_2\frac{\partial h}{\partial \theta}$$
$$-12\mu r U_2\frac{\partial H_1}{\partial r}-12\mu V_2\frac{\partial H_1}{\partial \theta}$$
$$+6\mu hr\frac{6U_2}{\partial r}+6\mu h\frac{6U_2}{\partial \theta}+6\mu h U_2+12\mu r W_2, \qquad (1)$$

where p is the pressure field, $h = H_2 - H_1$ is the film thickness, μ is the dynamic viscosity and U_2, V_2, W_2 are the velocity components of the points M_2 of the rotor.

The equation is solved using finite difference with the Gauss–Seidel method. The boundary conditions are the following:

- the feed pressure in each groove (atmospheric pressure) and
- the Christopherson assumption, i.e., negative pressures are set to zero at each iteration.

The force components and the moment components are calculated by integrating the pressure field into the surface S_2 of the rotor.

$$\mathbf{F}_b=\iint_{S_2}\mathbf{p}\,\mathrm{d}s, \qquad \mathbf{M}_b(\mathbf{O}_2)=\iint_{S_2}\mathbf{O}_2\mathbf{M}\wedge\mathbf{p}\,\mathrm{d}s \qquad (2,\ 3)$$

2.1.2. THRUST BEARING DEFECT

The defect of a thrust bearing is a wave in the rotor due to a manufacturing problem. For example, this defect can be generated by vibrations during the manufacturing process or it can be due to material relaxation after the manufacturing process. Figure 2 presents this

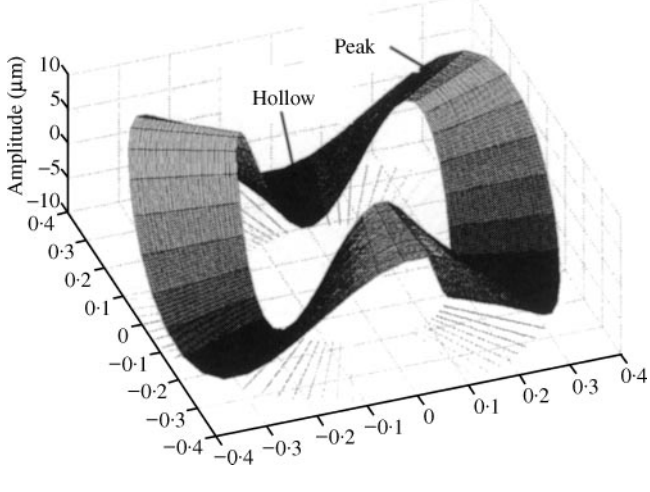

Figure 2. Thrust bearing defect (period $2\pi/3$).

wave for a period equal to $2\pi/3$. In this study, the period is equal to $2\pi/3$ and π. The amplitude of the defect is equal to 5, 10 and 15 μm. As explained in reference [6], the following phenomenon occurs. In the defective thrust bearing, the fluid film located between the stator and a peak of the wave on the rotor is thinner than the film near a hollow. Therefore, it creates a pressure peak which generates a dynamic bending moment on the rotor. This moment rotates with the defect. Thus, a levelness defect with n_w peaks generates a bending moment which excites the rotor at the frequency $n_w *$ shaft rotation frequency. Defects on the stator do not have the same influence: these defects create small static variations on the pressure which do not influence the shaft dynamic behaviour.

2.2. BEARING MODEL

The shaft is mounted on two identical hydrodynamic bearings whose dynamic behaviour can be modelled with dynamic coefficients. However, the dynamic coefficients are valid for a constant speed and in simulations the rotational speed varies from 3000 to 20 000 r.p.m. Thus, in order to calculate the bearing force, the thin film behaviour is assumed to be non-linear and then the film equation has to be solved using finite differences. However, the non-linear analysis of the shaft requires a large numerical calculation, and so the solution for a short bearing has been chosen. This assumption helps to simplify the differential equation; the circumferential flow is neglected. This is true when the length of the journal bearing remains small compared to its radius. The force components are obtained by integrating the pressure field with the following boundary conditions: the feed pressure on both sides of the bearing (atmospheric pressure) and the Gumbel assumption (π film), i.e., the negative pressure, are set to zero [5]. It must be noted that the finite length bearings can be used and the same phenomenon should occur.

2.3. SHAFT MODEL

2.3.1. *Lateral dynamic behaviour*

The rotor is modelled with typical beam finite elements including gyroscopic effects [14]. Each element has four degrees of freedom: two translations in the directions x_0 and y_0, and two axes of rotations (x_0 and y_0).

The differential system with $\{\boldsymbol{\delta}\}$ as the node displacement vector is

$$[\mathbf{M}]\{\ddot{\boldsymbol{\delta}}\} + [\mathbf{C}]\{\dot{\boldsymbol{\delta}}\} + [\mathbf{K}]\{\boldsymbol{\delta}\} = \{\mathbf{F}_{imb}\} + \{\mathbf{F}_{nl}\} + \{\mathbf{F}_{gr}\}, \tag{4}$$

where $[\mathbf{M}]$ is the mass matrix, $[\mathbf{C}]$ is the damping and gyroscopic matrix, $[\mathbf{K}]$ is the stiffness matrix, $\{\mathbf{F}_{imb}\}$ is the imbalance forces, $\{\mathbf{F}_{nl}\}$ is the non-linear bearing forces, $\{\mathbf{F}_{gr}\}$ is the gravity forces.

This system has $4n$ degrees of freedom (n is the number of nodes). To reduce the degrees of freedom, a modal approach is used by Lacroix [15] and Lalanne *et al.* [16]. The journal bearing is first modelled by a linear stiffness and then the fundamental principle of mechanics on the rotor could be written as

$$[\mathbf{M}]\{\ddot{\boldsymbol{\delta}}\} + ([\mathbf{K}_r] + [\mathbf{K}_{bearing}])\{\boldsymbol{\delta}\} = \mathbf{0}. \tag{5}$$

The solution has the following form: $\{\boldsymbol{\delta}\} = \{\boldsymbol{\delta}_0\}e^{rt}$ and the first six modes are calculated. Lacroix [15] has shown that six modes are enough to obtain an acceptable precision. A change of variable is made in the following form: $\{\boldsymbol{\delta}\} = [\boldsymbol{\psi}]\{\mathbf{q}\}$ with $[\boldsymbol{\psi}]$ the matrix obtained with modal vectors. $\{\boldsymbol{\psi}_i\}$ and $\{\mathbf{q}\}$ are the modal vectors of displacement. A new system is written where the bearing effect appears in the modal stiffness matrix, i.e.,

$$[\mathbf{m}]\{\ddot{\mathbf{q}}\} + [\mathbf{c}]\{\dot{\mathbf{q}}\} + [\mathbf{k}']\{\mathbf{q}\} = \{\mathbf{f}\}$$

with:

$$[\mathbf{m}] = [\boldsymbol{\psi}]^t[\mathbf{M}][\boldsymbol{\psi}], \qquad [\mathbf{c}] = [\boldsymbol{\psi}]^t[\mathbf{C}][\boldsymbol{\psi}],$$
$$[\mathbf{k}'] = [\boldsymbol{\psi}]^t[\mathbf{K}][\boldsymbol{\psi}], \qquad \{\mathbf{f}\} = [\boldsymbol{\psi}]^t\{\mathbf{F}\}. \tag{6}$$

For a non-linear calculation, the linear journal bearing effect $[\mathbf{K}_{bearing}]$ must be subtracted from the modal stiffness $[\mathbf{k}']$ and must be introduced as a non-linear effect.

Then

$$[\mathbf{m}]\{\ddot{\mathbf{q}}\} + [\mathbf{c}]\{\dot{\mathbf{q}}\} + [\mathbf{k}]\{\mathbf{q}\} = \{\mathbf{f}\} + \{\mathbf{F}nl\}$$

with

$$[\mathbf{k}] = [\mathbf{k}'] - [\boldsymbol{\psi}]^t[\mathbf{k}_{bearing}][\boldsymbol{\psi}]. \tag{7}$$

Note

1. The value of $[k_{bearing}]$ is difficult to select. Kassai [17] showed that it was necessary to take an intermediate value of bearing stiffness (for computing the modal basis). This is done to obtain a modal basis that allows for a displacement in the bearing nodes.
2. No material damping is considered.

2.3.2. *Axial dynamic behaviour*

In the axial direction (z_0), the shaft is considered rigid. Its dynamic behaviour is described by the following equation:

$$m\ddot{z} = F_{b_z} + F_a, \tag{8}$$

where m is the shaft mass, F_{b_z} is the axial force generated by the thrust bearing and F_a is an external axial force.

2.4. NON-LINEAR SIMULATION

The simulations of the axial dynamic behaviour and the lateral dynamic behaviour of the flexible rotor are independent. The only relation between these models is the thrust bearing. The coupling between fluid elements and the shaft is calculated using a non-linear approach. The simulation of the lateral behaviour of the flexible rotor is a step-by-step approach on a modal basis.

The flow chart is the following:

1. Begin with initial values of modal positions and velocities;
2. Calculation of external modal forces (imbalance, weight, etc.);
3. Calculation of physical displacements and velocities in bearings and thrust bearings (through modal basis change);
4. Calculation of non-linear bearing forces (in the real basis);
5. Calculation of non-linear thrust bearing forces and moments (in the real basis);
6. Computation of all forces in the modal basis (through modal basis change);
7. Calculation of modal accelerations (differential system);
8. Time integration (using the variable step Euler method);
9. Shaft speed incremented;
10. The process restarts from 2.

The simulation of the axial behaviour of the rotor is obtained using a similar process in the real basis (direction z_0).

3. RESULTS

3.1. DATA

The shaft is mounted on two identical bearings and a thrust bearing supports the axial load at one end. The model of the shaft is presented in Figure 3.

The thrust bearing has four pads. The data for each pad are the angle $\beta = 80$, the outer radius $R_2 = 0{\cdot}04$ m and the inner radius $R_1 = 0{\cdot}02$ m. The entry thickness h_e, the exit thickness h_s of each pad and the axial clearance of the thrust bearing are defined in relation to a virtual surface S (Figure 4). This surface S does not represent a real surface and it is used just as a position reference. The entry thickness h_e is equal to 55 μm and the exit thickness h_s is equal to 75 μm. The axial clearance is defined as the distance h_c between the centre of the surface S_2 and the surface S of the thrust bearing. In different simulations, it ranges from 100 to 160 μm.

The data for the journal bearings are the following: length $L = 0{\cdot}015$ m, radius $R = 0{\cdot}03$ m, radial clearance $C = 3{\cdot}0\text{E} - 05$ m and dynamic viscosity $\mu = 0{\cdot}05$ Pa s. (Figure 4) To quantify the damping and stiffness of journal bearings 1 and 2, the dynamic coefficients are given in Table 1.

3.2. SHAFT BEHAVIOUR

In this section, the bending vibrations of the shaft are studied.

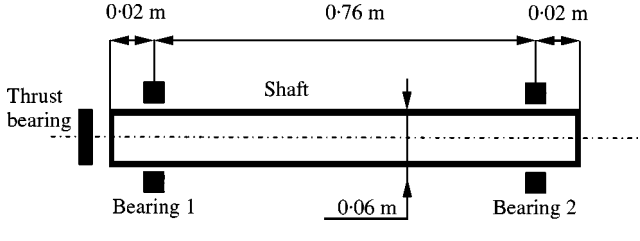

Figure 3. Geometrical data of the shaft.

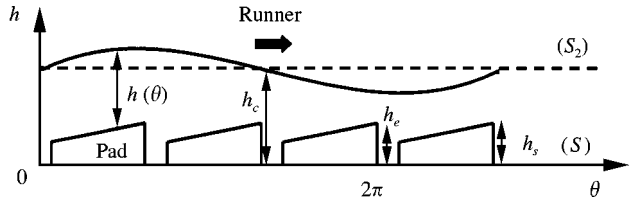

Figure 4. Film circumferential thickness in the thrust bearing.

TABLE 1

Damping and stiffness coefficients of the journal bearings

	Stiffness coefficients (N/m)				Damping coefficients (N s/m)			
	k_{xx}	k_{xy}	k_{yx}	k_{yy}	b_{xx}	b_{xy}	b_{yx}	b_{yy}
6000 r.p.m.	15 E+06	100 E+06	−90 E+06	30 E+06	300 E+03	40 E+03	40 E+03	300 E+03
12 000 r.p.m.	17 E+06	190 E+06	−190 E+06	33 E+06	300 E+03	27 E+03	27 E+03	300 E+03
18 000 r.p.m.	20 E+06	280 E+06	−270 E+06	30 E+06	300 E+03	10 E+03	10 E+03	280 E+03

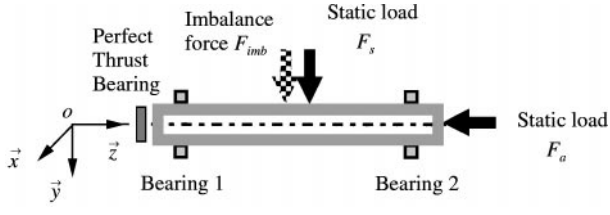

Figure 5. Rotating system: (⬬) dynamic force, (➡) static force. $\|\mathbf{F}_s\| = 800$ N; $\|\mathbf{F}_a\| = 2000$ N; $\|\mathbf{F}_{imb}\| = 1{\cdot}5\text{E} - 05$ kg m.

3.2.1. *Perfect thrust bearing and imbalance force*

The first calculation deals with the non-linear behaviour of the shaft with a perfect thrust bearing. In the middle of the rotor, an imbalance force excites the system and a static load is applied in order to stabilize it. Moreover, a perfect thrust bearing supports an axial static force (Figure 5).

Figure 6 presents the non-linear imbalance response of the shaft. The trajectory amplitude of the middle of the shaft is plotted in the plane (x_0, y_0).

Note: All the amplitudes given in this paper are non-dimensional (amplitude/bearing radial clearance ratio). The classical choice is to relate the shaft amplitude to the bearing radial clearance. This clearance corresponds to a maximum displacement of the shaft in its housing. Using this value as a reference is a good way to compare several results.

The first bending critical speed appears at 12 700 r.p.m. and the peak amplitude is equal to 0·45 times the bearing radial clearance. This imbalance response is a usual result.

3.2.2. *Defective thrust bearing and without imbalance force*

3.2.2.1. *Response of the shaft*. The influence of a defective thrust bearing on the dynamic behaviour of the shaft is studied. A static load is applied in the middle of the shaft and the defective thrust bearing supports an axial force. It must be pointed out that *no unbalance*

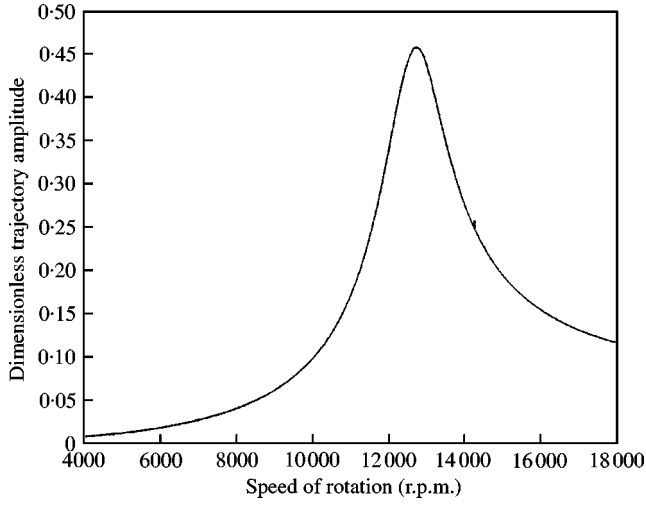

Figure 6. Non-linear imbalance response of the shaft middle with a perfect thrust bearing.

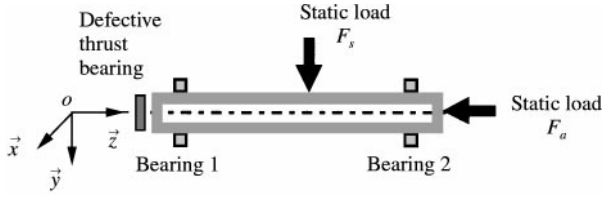

Figure 7. Rotating system: (▪▪▪) static force. $\|\mathbf{F}_s\| = 800$ N; $\|\mathbf{F}_a\| = 2000$ N.

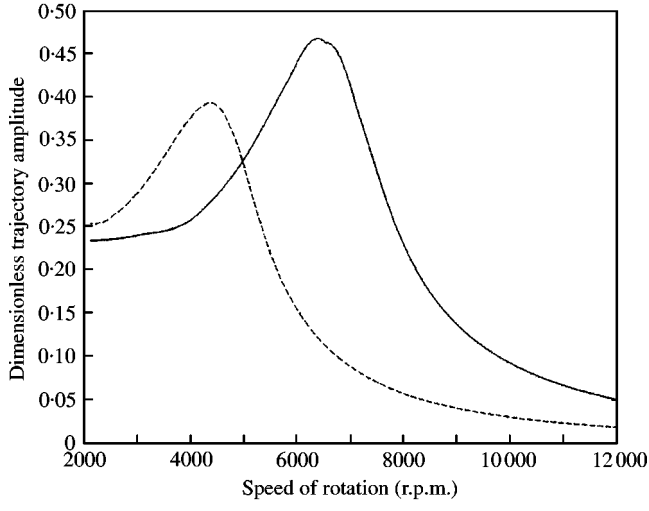

Figure 8. Response of the shaft with a defective thrust bearing and without imbalance force: (——) 2 waves; (- - - -) 3 waves.

force is applied on the shaft (Figure 7). The amplitude of the defect is equal to 10 μm and the period of the waves is π (two waves) and $2\pi/3$ (three waves).

Figure 8 displays the trajectory amplitude of the middle of the shaft for two periods of the waves (π and $2\pi/3$). When the period is equal to π, a new apparent critical speed appears at

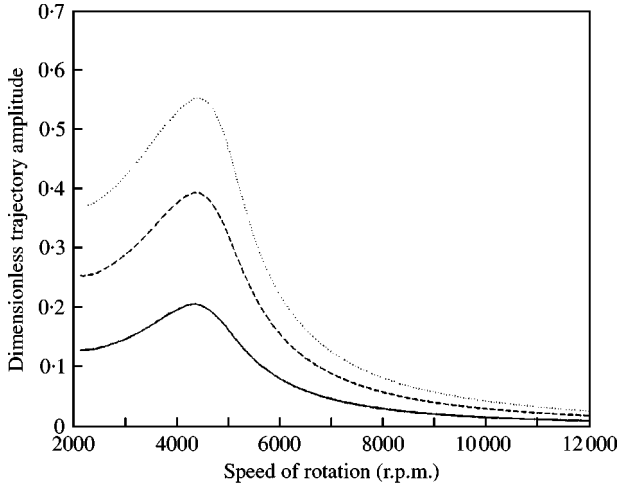

Figure 9. Response of the shaft with a defective thrust bearing—influence of the amplitude of the defect: (——) 5 μm; (- - - - -) 10 μm; (· · · · ·) 15 μm.

6400 r.p.m. and the peak amplitude is equal to 0·46 times the bearing radial clearance (c). When the period is $2\pi/3$, a new apparent critical speed is generated at a lower value (4300 r.p.m.) and the peak amplitude is smaller (0·4 C).

The values of the peak for a defective thrust bearing or an imbalance force of 1·5E − 05 kg m are equivalent. A levelness defect in a thrust bearing whose period is equal to $2\pi/m_w$ generates an apparent critical speed equal to first bending critical speed/n_w ratio. This apparent critical speed is due to the bending moment generated by the defect which excites the rotor at a frequency equal to $n_w *$ the shaft rotation frequency. It must be added that the smaller the number of defect waves, the higher the new critical speed and the more significant is the peak amplitude.

3.2.2.2. *Influence of the amplitude of the defect*. The influence of the amplitude of the defect on the dynamic behaviour of the shaft is analyzed. Three simulations are made for the previous rotating system. The amplitude of the defect is equal to (successively) 5, 10 and 15 μm. Figure 9 shows the response of the middle of the shaft. The higher the amplitude of the defect, the more significant is the peak amplitude. Thus, a slight defect (15 μm; that is, about rotor thickness $* 10^{-3}$) can generate a peak whose amplitude is equal to 54% * radial bearing clearance.

3.2.2.3. *Influence of the axial load*. The effect of the axial load on the amplitude of the shaft vibrations is examined. Figures 10 and 11, respectively, present the trajectory amplitude of the middle of the shaft and the axial clearance of the thrust bearing, when the axial load successively is equal to 500, 100 and 2000 N.

The heavier the axial load, the more significant are the amplitudes of vibrations, because the heavier the axial load, the smaller the axial clearance of the thrust bearing and the higher the amplitude of the defect/axial clearance of the thrust bearing ratio (Figure 11). It is an interesting result because, on the contrary, when an imbalance force only excites the shaft (perfect thrust bearing), the heavier the axial load, the less significant are the amplitudes of vibrations [18]. Thus it is not easy to adjust the axial load in order to decrease the amplitudes of the vibrations of the shaft.

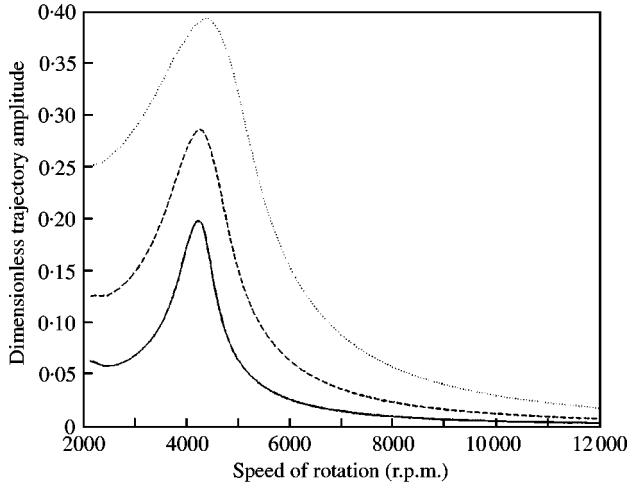

Figure 10. Response of the shaft with a defective thrust bearing—influence of the axial load: (——) 500 N; (- - - - -) 1000 N; (· · · · ·) 2000 N.

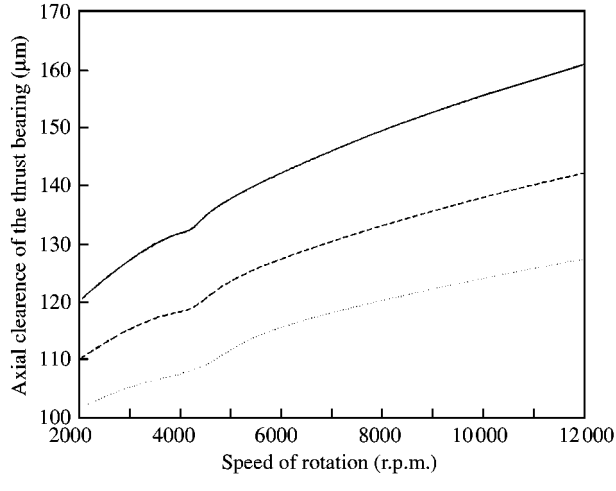

Figure 11. Response of the shaft with a defective thrust bearing—influence of the axial load: (——) 500 N; (- - - - -) 1000 N; (· · · · ·) 2000 N.

3.2.3. *Defective thrust bearing & imbalance force*

The calculation deals with the behaviour of the shaft with a defective thrust bearing (10 μm, $2\pi/3$). Moreover, in the middle of the rotor, an unbalance force excites the system (Figure 12).

Figure 13 displays the response at the middle of the shaft. Two peaks of vibrations at 4300 and 12 700 r.p.m. appear. The first peak (4300 r.p.m.) is generated by the defect in the thrust bearing and the second peak (12 700 r.p.m.) is due to the imbalance force which excites the first bending critical speed. The amplitudes of the peaks are the same in comparison with the "defective thrust bearing" case and the "perfect thrust bearing & imbalance force" case. In experiments, a sub-critical peak may sometimes be observed. This type of levelness defect would be able to explain this subcritical speed.

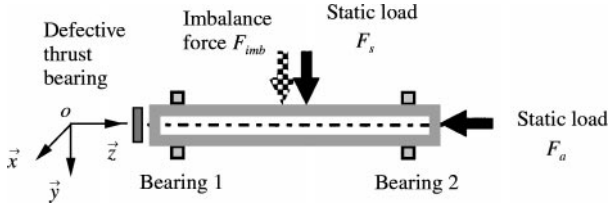

Figure 12. Rotating system: (▪▪▪) dynamic force; (▬▶) static force. $\|\mathbf{F}_s\| = 800$ N; $\|\mathbf{F}_a\| = 2000$ N; $\|\mathbf{F}_{imb}\| = 1{\cdot}5\text{E} - 05$ kg m.

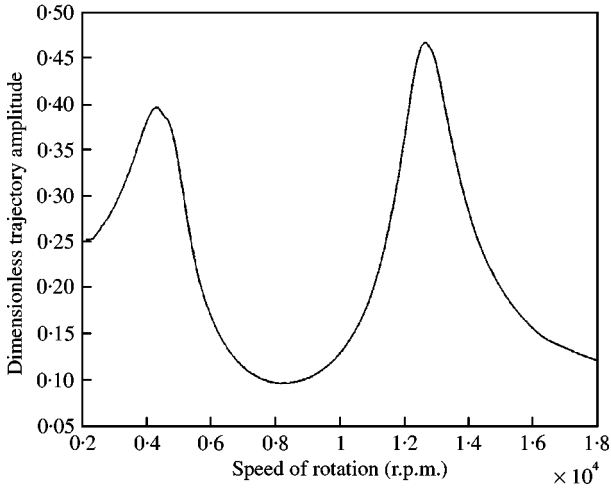

Figure 13. Response of the shaft with a defective thrust bearing and an imbalance force.

4. CONCLUSION

The influence of the dynamic behaviour of a defective thrust bearing on the bending vibrations of a flexible shaft can be strong. A small levelness defect in a thrust bearing whose period is equal to $2\pi/n_w$, generates a new apparent critical speed equal to the first bending critical speed/n_w ratio. This apparent critical speed is due to the bending moment generated by the defect which excites the rotor at a frequency equal to $n_w *$ the shaft rotation frequency. The smaller the number of defect waves, the more significant are the amplitudes of vibration. The influence of the axial load on the amplitude of the shaft vibrations is important. The heavier the axial load, the more significant are the amplitudes of vibrations. The amplitudes of vibrations generated by a levelness defect in a thrust bearing can be equivalent to the vibrations due to an imbalance force. It must be pointed out that the linear approach is unable to show the supplementary critical speeds which are obtained only by using non-linear analysis for the thrust bearing: the film thickness in the thrust bearing varies each time (due to the rotor defects) and it is impossible to linearize the film behaviour by stiffness and damping coefficients. The phenomenon is due to the pressure field which rotates with the shaft and excites its first natural frequency. In fact, it appears more as a new excitation frequency than a new critical speed, linear model cannot be applied but the physical phenomenon is almost linear.

REFERENCES

1. B. FANTINO 1973 *Thèse de Doctorat de Spécialité Mécanique, Lyon.* Influence des défauts de formes dans la lubrification hydrodynamique.
2. B. FANTINO and J. FRÊNE 1975 *Matériaux Electricité Revue du GAMI* **308–309**, 40–44. Charge tournante et défauts de forme en régime transitoire Mécanique.
3. D. BERTHE, B. FANTINO, J. FRÊNE and M. GODET 1974 *Journal of Mechanical Engineering Science, Institution of Mechanical Engineers* **16**, 156–159. Influence of the shape defects and surface roughness on the hydrodynamics of lubricated systems.
4. D. BERTHE and M. GODET 1971 *C. R. Académie des Sciences, Paris* **272**, 1010–1013. Equation de l'écoulement laminaire entre deux paroix rapprochés en mouvement relatif.
5. O. BONNEAU and J. FRÊNE 1996 *International Journal of Rotating Machinery* **2**, 281–287. Influence of bearing defects on dynamical behaviour of an elastic shaft.
6. P. L. JIANG and L. YU 1988 *Mechanics Research Communications* **25**, 219–224. Effect of a hydrodynamic thrust bearing on the statics and dynamics of a rotor-bearing system.
7. N. MITTWOLLEN, T. HEGEL and J. GLIENICKE 1991 *Journal of Tribology* **113**, 881–818. Effect of hydrodynamic thrust bearings on lateral shaft vibrations.
8. S. BERGER, O. BONNEAU and J. FRÊNE 1998 *Proceedings of the 5th International Tribology Conference Austrib* '98, *Brisbane*, 6–9 December, 389–394. Influence of axial thrust bearing defects on the dynamic behavior of an elastic shaft.
9. G. A. LABOUFF and J. F. BOOKER 1985 *Transactions of the American Society of Mechanical Engineers Journal of Tribology*, **4**, 505–515. Dynamically-loaded journal bearings. A finite element treatment for rigid and elastic surfaces.
10. B. FANTINO, J. FRÊNE and J. DU PARQUET 1979 *Transactions of American Society of Mechanical Engineers JOLT* **101**, 190–200. Elastic connecting-rod bearing with piezoviscous lubricant: analysis of the steady-state characteristics.
11. R. DESAILLY, B. FANTINO and J. FRÊNE 1978 *Fifth Leeds–Lyon Symposium on Tribology, Leeds, England*, September. *Proceedings of the IME* "*Elastohydrodynamics and related topics*', 1979, 329–336. Hydrodynamics of an elastic connecting rod bearing: comparison of theoretical and experimental results.
12. J. PIERRE-EUGÉNE, J. FRÊNE, B. FANTINO, G. ROUSSEL and J. DU PARQUET 1983 *Ninth Leeds–Lyon Symposium on Tribology. Tribology of Reciprocating Engines*, 49–54. London: *Butterworths.* Theory and experiments on elastic connecting rod bearings under steady state conditions.
13. G. GOODWIN and R. HOLMES 1982 *Tribology-Key to the Efficient Engine, Institute of Mechanical Engineers Conference Publications, Paper* C2/82, 9–15. Bearing deformation and temperature distribution in dynamically-loaded engine bearings.
14. O. BONNEAU, A. KASSAI, J. FRÊNE and J. DER HAGOPIAN 1989 *Proceedings of the EUROTRIB, Helsinki, Finland*, June, Vol. 4, 145–149. Dynamical behavior of an elastic rotor with a squeeze film damper.
15. J. LACROIX 1988 *Thèse de Doctorat de l'INSA de Lyon.* Comportement dynamique d'un rotor au passage des vitesses critiques.
16. M. LALANNE and G. FERRARIS 1990 *Rotordynamics Prediction in Engineering.* Chichester: Wiley.
17. A. KASSAI 1989 *Thèse de l'INSA de Lyon.* Contribution à l'Etude Dynamique des rotors Amortis.
18. S. BERGER 1999 *Thèse de doctorat de l'Université de Poitiers.* Etude du comportement dynamique non linéaire d'un rotor monté sur éléments fluides: caractérisation des étanchéités—influence de la butée.

APPENDIX A: NOMENCLATURE

(o_0, x_0, y_0, z_0)	fixed reference
(o_0, r, t, z_0)	local reference
(o_1, x_1, y_1, z_1)	reference fixed to the thrust bearing rotor
(o_2, x_2, y_2, z_2)	reference fixed to the thrust bearing stator
p	pressure field (Pa)
h	film thickness (m)
U_2, V_2, W_2	velocity components of the thrust bearing rotor in the reference (o_0, r, t, z_0) (m/s)
μ	dynamic viscosity (Pa s)

r	radial parameter (m)
θ	angular parameter being its origin on the axis x_0
β	angle of each thrust bearing pad (°)
R_1	outer radius of pad thrust bearing (m)
R_2	inner radius of pad thrust bearing (m)
h_e	entry thickness of pad thrust bearing (m)
h_s	exit thickness of pad thrust bearing (m)
h_c	thrust bearing axial clearance (m)
n_w	number of waves: the period of the defect is $2\pi/n_w$
F_{b_z}	thrust bearing axial force (N)
C	radial clearance (m)
L	bearing length (m)
R	bearing radial clearance (m)
m	shaft mass (kg)
n	number of nodes
$\{\boldsymbol{\delta}\}$	node displacement (m)
$[\mathbf{C}]$	damping and gyroscopic matrix (N s/m)
$[\mathbf{K}]$	stiffness matrix (N/m)
$[\mathbf{K}_{bearing}]$	bearing stiffness (N/m)
$k_{xx}, k_{xy}, k_{yx}, k_{yy}$	bearing stiffness coefficients (N/m)
$b_{xx}, b_{xy}, b_{yx}, b_{yy}$	bearing damping coefficients (N s/m)
$[\mathbf{M}]$	mass matrix (kg)
$[\boldsymbol{\psi}]$	modal matrix
$\{\mathbf{F}_{imb}\}$	imbalance forces (N)
$\{\mathbf{F}_{nl}\}$	non-linear bearing forces (N)
$\{\mathbf{F}_{gr}\}$	gravity forces (N)
F_s	static lateral axial load (N)
F_a	external axial force (N)
N_a	rotational shaft frequency (Hz)